Diversity of fate outcomes in cell pairs under lateral inhibition

Nara Guisoni[1,2], Rosa Martinez Corral[1], Jordi Garcia Ojalvo[1,#], and Joaquín de Navascués[3,#]

[1] Department of Experimental and Health Sciences, Universitat Pompeu Fabra, Barcelona Biomedical Research Park (PRBB), Dr. Aiguader 88, 08003 Barcelona, Spain.

[2] Instituto de Física de Líquidos y Sistemas Biológicos, CONICET & Universidad Nacional de La Plata, Calle 59-789, 1900 La Plata, Argentina.

[3] European Cancer Stem Cell Research Institute, School of Biosciences, Cardiff University, Hadyn Ellis Building, Maindy Road, Cardiff CF24 4HQ, UK.

[#] Correspondence: denavascuesj@cardiff.ac.uk, jordi.g.ojalvo@upf.edu

Abstract

Cell fate decision making mediated by lateral inhibition via Notch/Delta signalling has been extensively studied, both experimentally and theoretically. Most formalised models consider Notch-Delta interactions among many cells, usually in periodic arrangements, with parameters leading to a dynamical behaviour that typically results in symmetry breaking of signalling states between neighbouring cells. This leads to patterns of sparse cells with distinct fates, whose relative spacing is a measure of the developmental output. Here we consider the case of signalling between isolated cell pairs, and find that the bifurcation properties of a standard mathematical model of Notch/Delta signalling can lead to stable symmetric states, with either the two cells activating the Notch receptor, or both expressing the Delta ligand. This model is directly relevant to the regulation of adult stem cell fate, which is often determined by Notch/Delta interactions. We apply this model to the homeostatic replacement of the adult *Drosophila* intestine, where the fate outcome of intestinal stem cell (ISC) division is stochastic but dependent on the Notch/Delta pathway. Our experiments show a correlation between cellular fate in pairs of progenitor cells and the contact area between them. We interpret this behaviour in terms of the bifurcation properties of our model in the presence of population variability in signalling thresholds. Our results suggest that the dynamics of Notch/Delta signalling can contribute to explain the stochastic balance of cell fate decisions after ISC division, and that the standard model for lateral inhibition is able to account for a wider range of developmental outcomes than checkerboard-like patterning.

Introduction

The Notch/Delta signalling pathway is one of the main regulators of cellular differentiation during development and adult tissue maintenance (reviewed in Artavanis-Tsakonas et al., 1999; Ehebauer et al., 2006; Koch et al., 2013). It often drives mutually inhibitory interactions between cells, acting as a gate for differentiation. This mode of action has been termed lateral inhibition and has been the object of experimental study as well as mathematical formalisation for decades (see, for instance, Othmer and Scriven, 1971; Collier et al., 1996; Sprinzak et al., 2011; Petrovic et al., 2014). Quantitative models of lateral inhibition usually involve a field of cells expressing initially similar amounts of the receptor Notch and its membrane-bound ligand Delta. Delta trans-activates Notch in neighbouring cells and Notch, once activated, reduces in turn the ability of the cell to signal through Delta, leading to a state of metastable mutual repression. This symmetry (and cell fate equivalence) is eventually broken by enforced biases and/or stochastic variation in Notch/Delta levels (Collier et al., 1996; Plahte, 2001; reviewed in Simpson, 2001). These models usually relate to real developmental systems that result in extended fine-grained spacing patterns (Othmer and Scriven, 1971; Collier et al., 1996; see also Shaya and Sprinzak, 2011) and have been experimentally characterized in depth (reviewed in Greenwald, 1998; Arias and Stewart, 2002). Little attention has been paid so far to the effect of lateral inhibition in isolated cell pairs, beyond the trivial expectation that symmetry breaking will eventually take place, leading to cells taking opposing fates (see for instance Collier et al., 1996; Rouault and Hakim, 2012). However there has been no formal investigation of whether alternative steady states are possible, perhaps due to the lack of an experimental model to relate it to.

The cellular homeostasis of the adult *Drosophila* midgut can provide this experimental scenario, as in this tissue Notch/Delta signalling occurs mostly in isolated pairs of cells (Ohlstein and Spradling, 2006; de Navascués et al., 2012) (Figure 1A). The fly's intestinal lining is maintained by intestinal stem cells (ISCs), which divide to both self-renew and provide committed progenitors. These progenitors, commonly referred to as enteroblasts (EBs), eventually replace differentiated cells lost by wear and tear (Figure 1B). (Note that we are referring to EBs as the committed progeny of the ISC, irrespective

of their terminal differentiation choice.) Undifferentiated cells (ISCs and EBs) are frequently found in pairs, which are thought to result from the division of an ISC and subsequent fate allocation, before a new division or terminal differentiation event takes place (Goulas et al., 2012; de Navascués et al., 2012). ISC divisions are resolved stochastically, resulting in either asymmetric fate (one ISC and an EB), or symmetric self-renewal (two ISCs) or differentiation (two EBs) in balanced proportions (de Navascués et al., 2012) (Figure 1C). This mode of tissue maintenance, whereby the balance between stem cell self-renewal and differentiation is achieved at the population level rather than within every stem cell lineage, is termed neutral competition (Klein and Simons, 2011) and is found in a growing number of self-renewing adult tissues (Simons and Clevers, 2011). While no molecular mechanism has been fully elucidated so far for any case of neutral competition, in the fly gut it has been proposed to arise from lateral inhibition mediated by Notch/Delta (de Navascués et al., 2012), a pathway known to define the fate of the ISC offspring (Ohlstein and Spradling, 2006; Micchelli and Perrimon, 2006; Bardin et al., 2010).

Here we explore the capacity of a standard model of lateral inhibition acting in pairs of interacting cells to result in steady states with different signalling states (either symmetric or asymmetric) coexisting in the tissue. We find that this is indeed possible, provided there is population-wide variation of signalling thresholds. Next, we turn to the *Drosophila* midgut and find that the tissue displays high variability of contact area between pairs of ISC/progenitor cells, which seems to result in an effective heterogeneity in signalling thresholds between pairs of cells. When contrasting this variability with the distribution of fate combinations in pairs of ISC/EB cells, we find a correlation between contact area of specific cell pairs and their fate profile. Moreover our model is able to reproduce the distribution of fate outcomes given the contact area distribution.

Our results expand the repertoire of possible outputs of a system governed by lateral inhibition and connect this mode of signalling with a mode of stem-cell based tissue maintenance (neutral competition), which is highly relevant in adult tissue homeostasis and tumorigenesis (Simons and Clevers, 2011;

Vermeulen et al., 2013; Baker et al., 2014; Vermeulen and Snippert, 2014) and whose molecular regulation is poorly understood.

Methods

The model: lateral inhibition mediated by Notch-Delta interaction

We consider that the rate of Notch activation in a cell is an increasing function of Delta concentration on its neighbour (signalling), and that the rate of Delta expression is a decreasing function of the level of activated Notch in the same cell (inhibition). We represent these interactions by means of a standard mathematical model of Notch/Delta signalling (Collier et al., 1996) between pairs of cells, which is given by:

$$\frac{dN_1}{dt} = \alpha f(D_2) - \delta_N N_1, \tag{1}$$

$$\frac{dD_1}{dt} = \beta g(N_1) - \delta_D D_1, \tag{2}$$

$$\frac{dN_2}{dt} = \alpha f(D_1) - \delta_N N_2, \tag{3}$$

$$\frac{dD_2}{dt} = \beta g(N_2) - \delta_D D_2. \tag{4}$$

Here $N_{1,2}$ represent the levels of Notch activity in cells 1 and 2, $D_{1,2}$ is the concentration of Delta in each cell. α and β are the maximal production rates of Notch and Delta, respectively, whereas δ_N and δ_D are their corresponding degradation rates. The production terms for Notch (*f*) and Delta (*g*) are given by the Hill functions

$$f(x) = \frac{x^r}{K_N^r + x^r}, \qquad g(x) = \frac{1}{1+(x/K_D)^h}, \tag{5}$$

where the former function represents the signalling effect of Delta on the neighbouring cell, and the latter corresponds to the inhibition of Delta expression by activated Notch in the same cell. K_N is the threshold of Notch activation by neighbouring Delta, K_D is the threshold of Delta inhibition by Notch in the same cell, and the coefficients *r* and *h* represent the cooperative

character of the two aforementioned processes. Also, following (Collier et al., 1996) we define two dimensionless parameters *a* and *b,* which set the location of the half-maximal point of the sigmoidal curves of equation (5) in the dimensionless version of equations (1)-(4), and are referred to as the activation and inhibition thresholds, respectively:

$$a \equiv \frac{K_N \delta_D}{\beta}, \qquad b \equiv \frac{K_D \delta_N}{\alpha} \tag{6}$$

<u>*Steady states and cell fate identification*</u>

The system of equations (1)-(4) has a homogeneous steady state in which Notch and Delta have the same values in the two cells:

$$N^* = \frac{\alpha}{\delta_N} f(D^*), \qquad \mathrm{D}^* = \frac{\beta}{\delta_D} g(N^*)$$

This state corresponds to a situation in which both cells in the pair have the same fate. The stability boundary of this homogeneous steady state can be calculated using standard methods (Collier et al., 1996), and is represented by a dotted grey line in Figure 2A. Above this line the homogeneous state is stable. Below it, a heterogeneous stable steady state appears in which the values of Notch and Delta are different between the two cells:

$$N_1^* = \frac{\alpha}{\delta_N} f(D_2^*), \qquad D_1^* = \frac{\beta}{\delta_D} g(N_1^*),$$

$$N_2^* = \frac{\alpha}{\delta_N} f(D_1^*), \qquad D_2^* = \frac{\beta}{\delta_D} g(N_2^*),$$

In parallel with this classification of steady states, a cell is considered to be Notch positive when the level of Notch surpasses a certain threshold N_{thr} (considered to be 0.1), and Notch negative in the opposite case. In the case of the *Drosophila* midgut, a Notch positive cell would correspond to an EB, and a Notch negative cell to an ISC. In that way, a homogeneous steady state can represent either an ISC/ISC pair (symmetric Notch negative) or an EB/EB pair (symmetric Notch positive). Most heterogeneous steady states, in turn, correspond to an ISC/EB pair, although heterogeneous states in which both values of Notch lie below (or above) the threshold N_{thr} still represent symmetric ISC/ISC (or EB/EB) pairs. This is reflected in Figure 2A through the

difference between the stability boundary (dotted grey line) and the boundaries between the fate-pair domains shown in colour code.

Dynamical behaviour

We investigate the temporal evolution of the model by solving numerically the dimensionless versions of Equations (1)-(4). For this purpose we use a finite difference approximation (two-stage Runge-Kutta; LeVeque, 2007). Cells are considered initially as negative for Notch activation, with similar initial levels of Notch and Delta ($N_1(t=0)=0.05$, $N_2(t=0)=0.06$, $D_1(t=0)=0.90$, $D_2(t=0)= 0.91$).

Drosophila culture and strains

Adult flies were raised in standard cornmeal medium, collected daily and maintained in fresh vials with added yeast (food replaced every 24-48h) until dissection at 4-6 days of age.

EBs were identified by co-expression of an enhancer trap reporter of the undifferentiation marker *escargot* (*esg*^{YB0232}; Quiñones-Coello et al., 2007) and the synthetic Notch transcriptional activity reporter *GBE-Su(H)-LacZ* (Bray and Furriols, 2001), while ISCs were identified by expression of the *esg* reporter alone (Micchelli and Perrimon, 2006; Ohlstein and Spradling, 2006) (Figure 1A).

Immunohistofluorescence and imaging

Immunofluorescence was performed essentially as described in (Bardin et al., 2010) but with a heat-fixation step (Miller et al., 1989).

Primary antibodies were: chicken anti-*β*-Galactosidase (Abcam ab9361, 1:200), rabbit anti-GFP (Abcam ab6556, 1:200), anti-Arm (mAb N2-7A1, Developmental Studies Hybridoma Bank, 1:50), sheep anti-Notch (Muñoz-Descalzo et al., 2011) 1:1000). Secondary antibodies conjugated with Alexa fluorophores were from Invitrogen (1:500).

Confocal stacks were obtained in a Zeiss LSM 710 with an EC Plan-Neofluar 40X oil immersion objective (numerical aperture 1.3), with voxel size 0.21x0.21x1.00 or 0.14x0.14x0.42 *μ*m (XYZ) for the quantification of contact area (with no oversampling in Z) and Notch distribution, respectively.

Image analysis

To measure contact area, stacks were analysed with a combination of ImageJ macros and python scripts to (1) manually identify all esg-GFP$^+$ cells in a z-projection of the stack, (2) automatically threshold *GBE-Su(H)-lacZ* reporter expression in 3D to determine its expression status (positive or negative) in every esg$^+$ cell, (3) manually identify the nests of esg$^+$ cells so that (4) a series of 3D stacks, containing each one pair only, is automatically cropped, and (5) the contact membrane of each esg$^+$ cell pair is semi-automatically determined using FIJI for each optical plane, by binarising the immunofluorescence of Armadillo/*β*-catenin (Arm). Arm labels the membrane throughout the apical-basal axis (see Results), which allows measuring the amount of contacting membrane in each cell pair as the number of Arm$^+$ voxels shared between the two cells (expressed in μm^2).

For measuring Notch and Arm distribution at the membrane, the membrane contours (3 pixels wide) of cells in pairs were manually determined in each plane. Intensity data from those positions were used as follows:

Intensity normalisation. For each cell pair, two nearby 50x50 pixel squares spanning the full z-stack were manually selected, the signal therein averaged for all the planes where membrane was detectable, and this average value taken as background. Notch and Arm intensity values for that stack were normalised by dividing by the background value.

Distribution along cell perimeter. Each membrane pixel position was assigned an angular value respect to the centroid by calculating its tangent arc (±π depending on the quadrant). Thirty overlapping sliding windows (of 2π/15 rad with half window overlap) were delimited in each plane, and their pixel intensities were normalised and averaged.

Distribution along the apical-basal axis. Each cell was sliced in 10 overlapping angular windows (2π/5 rad with half overlap). For each window, a normalised, average intensity measurement was taken per confocal plane (i.e. along the apical-basal axis). Apical-basal positions were normalised from 0 to 1. Intensity data points along the apical-basal axis were obtained by interpolation from average normalized intensity values.

Results

Lateral inhibition can result in stable, opposing symmetric signalling states

We study the steady-state behaviour of a standard model of lateral inhibition for the case of two cells (see Materials and Methods). The steady states of the system depend only on two parameters, a and b (the activation and inhibition thresholds, respectively; see Materials and Methods), which we allow to vary across the population of cell pairs. We then calculate the equilibrium state of the system in this two-dimensional parameter space, according to the resulting signalling profile: asymmetric (one cell positive for Notch activation and the other one negative, see Material and Methods), symmetric positive, or symmetric negative for Notch activation (Figure 1E). Thus, for a population of cell pairs with variable activation or inhibition thresholds (a and b), the three possible signalling state profiles occur (Figure 2A, see Figure 2C-E for a comparison of the dynamic evolution of examples of the three profiles with Figure 2B, with parameter values from Collier et al., (1996)). The three signalling state profiles can be found within a relatively short range of parameter values (Figure 2A), and this scenario does not change qualitatively when considering a wide range of threshold values for Notch activity classification, as defined in the Materials and Methods section ($0.001 \leq N_{thr} \leq 0.7$) (Supplementary Figure 1A-D).

In a biological system, the existence of three possible signalling state profiles would be equivalent to having three different cell fate combinations across a population of initially uncommitted cell pairs interacting through Notch/Delta, with the specific fate combination of a given cell pair depending on the sensitivity to Delta activation and Notch inhibition of the pair. To investigate the potential of this lateral inhibition model, incorporating variable activation and inhibition thresholds, to describe a real biological system, we turned to the *Drosophila* midgut.

Cell contact area as indicator of activation threshold

In the *Drosophila* midgut, Notch negative cells correspond to ISCs, and Notch positive to EBs. The Notch activity reporter *GBE-Su(H)* is hardly expressed above background levels in ISCs (Ohlstein and Spradling, 2007) and our own

observations), and hence our choice of a low threshold value, $N_{thr} = 0.1$. Symmetric positive pairs will equate to an event of symmetric differentiation (EB/EB), symmetric negative pairs to symmetric self-renewal (ISC/ISC) and asymmetric pairs to asymmetric ISC fate (ISC/EB) (Figure 2A).

To relate the model to real tissue, we need first to consider how the biochemical parameters a and b are related to biological features displaying variability across undifferentiated (esg$^+$) cell pairs. We assume that biochemical processes intrinsic to the cell, such as protein degradation rates (δ_D and δ_N), the maximal biosynthesis rates (α and β), or the threshold of Delta inhibition by Notch in the same cell (K_D), will not be highly variable among cells with a common developmental identity. On the other hand, the threshold of Notch activation by neighbouring Delta (K_N) depends directly on the interaction between the two cells, which could be variable for different pairs of cells. For instance, due to the spatial constraints of cell packing, the contact area between cell pairs could be substantially different from pair to pair. By looking at the tissue, it seems that undifferentiated cells in nests show irregular shapes and variable contact area (Figure 3A). If the amount of Notch available for signalling is limiting (which is generally true for the N/Dl system in *Drosophila* and has been observed in the gut (de Navascués et al., 2012; Biteau et al., 2008), and Notch receptors are randomly distributed throughout the cell membrane (see below), a smaller contact area between two cells will imply that a higher concentration of Delta is required in one cell for Notch to activate in the other cell (Khait et al., 2015). In terms of our model, this translates into a higher activation threshold of Notch by Delta, i.e. a higher value of K_N and therefore of a (Equation 6). We also note that a is the parameter whose variation best allows for heterogeneity in stable steady state levels of Notch activity, which will ultimately govern fate choice (Supplementary Figure 2B, compare with panels A, C, D), and therefore seems suitable as a control parameter. From this we conclude that variation of contact area (or any other biological feature correlating with the threshold of Notch activation a) is likely to allow the diversity in fate outcome that we observe in the model. Thus we can assume, in a first approximation, that the activation threshold a and the contact area are inversely related.

For this relationship to hold, Notch must be randomly distributed at the cell membrane. To evaluate this, we examined the localisation of both Notch and Armadillo/*β*-catenin (Arm) in both single and paired undifferentiated cells (recognised by *Notch* expression; Bardin et al., 2010) of the adult posterior midgut epithelium with confocal microscopy (Figure 3A). Arm is found in epithelial cells mostly at the adherens junctions (Tepass et al., 2001). Using Arm as a membrane marker, we defined membrane boundaries in 3D, and measured the intensity of Notch and Arm signals at the cell membrane.

We could not find any strong pattern in the variations of Notch immunodetection intensity within confocal planes, and it would only seem that Notch is slightly enriched at the boundary between two esg$^+$ cells (Figure 3B). This indicates that Notch concentration is largely independent of the position at the membrane along the cell perimeter, and in particular along the contact between esg$^+$ cells. Moreover, the localisation of Notch along the apical-basal axis of the cells is also largely homogeneous. This is manifest in the small variation in the average amounts of Notch between different optical planes (Figure 3D), and in the narrow distribution of mean values per plane, with low values of coefficients of variation per plane, of Notch intensity values (Supplementary Figure 3B,D). Therefore, the area of contact between cells is a good approximation to the total amount of Notch receptor available for signalling.

We note that Arm largely parallels Notch localisation at the membrane (Figure 3C,E and Supplementary Figure 3A,C) but shows a stronger enrichment at the boundary (Figure 3C), in agreement with previous reports (Maeda et al., 2008). Incidentally, these results also reveal that neither Arm nor Notch are restricted to the apical domain in the midgut epithelium**,** and instead can be found in similar amounts along the apical-basal axis of the membrane in ISCs and EBs (Figure 3D-F). This situation contrasts sharply with Arm and Notch distribution in other *Drosophila* epithelia (Tepass et al., 2001; Sanders et al., 2009).

Taken together, our results suggest that Notch receptor is randomly distributed in the cell membrane, which suggests that measurements of

membrane contact area may be relevant to the dynamics of Delta-Notch signalling as a proxy for the activation threshold a in our model.

Correlation of contact area values and cell fate profiles

We have shown that contact area can be used as a measure of the amount of Notch available for interaction with Delta. We thus measured contact area in 508 pairs of esg$^+$ cells with both symmetric (ISC-ISC and EB-EB) and asymmetric (ISC-EB) fates (Figure 1D-E); these pair classes have been described in (de Navascués et al., 2012; Goulas et al., 2012). We found the contact area in these pairs to be highly variable, ranging from just around 1μm^2 to over 60μm^2 (Figure 4A) and with a high coefficient of variation (0.52). This degree of variability indicates that contact area has the potential to be a regulatory mechanism of the system (through its influence on the activation threshold a).

Our model predicts that a biological feature influencing Notch/Delta signalling thresholds in cell pairs should correlate with the patterns of symmetric and asymmetric fates. Therefore, we classified measurements of contact area according to the fate profile of their corresponding cell pair and compared their values (Figure 4B). We found that on average, the contact area between ISC-ISC (11.59 ± 0.73 μm^2; mean ± standard error of the mean) is clearly smaller than those of ISC-EB (17.68 ± 0.42 μm^2) and EB-EB pairs (21.6 ± 2.76 μm^2). This is also clear when considering the distribution of sizes for each pair type and confirmed by the Kolmogorov-Smirnov test (Figure 4C). From these results we take that ISC-ISC pairs have a significantly smaller contact area than the other two fate profiles.

Updating the model with area variation reproduces fate profile distributions

This finding gives us biological justification to consider the activation threshold a variable in the model (inversely proportional to the contact area) and test the capacity of the model to produce the observed proportions of fate pairs. To do this, we first generated a large sample of contact area values A, from a Smooth Kernel Distribution based on the experimental data (Figure 4A). To input values from A into the model, we considered the area values A inversely related to the activation threshold a by a constant c (a=c/A), treated as a

parameter of the model. We then analysed the stable steady states of the model, obtaining the proportions of the three possible fate pairs resulting from A, for different values of b and c.

In order to compare the fate distribution obtained from the model and the experimental data we use the Kullback-Leibler relative entropy (H), which is a dissimilarity measure between two probability distributions (giving the value 0 if the distributions are equal; Kullback and Leibler, 1951). We found an excellent agreement between the proportions of EB-EB, EB-ISC and ISC-ISC pairs observed experimentally, and the distributions from the model for an extended range of values of b and c, as indicated by the low values of H between theoretical and experimental distributions (Figure 4D). The best fit (Table 1) is obtained with b=0.19 and c=18 (H=0.3×10^{-3}, black dot in Figure 4D). By mapping A input values (Figure 4A) for b=0.19 and c=18 to the model phase diagram (horizontal line in Figure 2A), one finds that ISC-ISC pairs occur at the lowest values of contact area, in good agreement with our experimental observations (Figure 4B-C). In this region of the parameter space, EB-EB and ISC-EB pairs are found at intermediate or high values of contact area (lower a), respectively. While the model favours EB-EB pairs resulting from smaller contact areas than ISC-EB pairs, we cannot distinguish statistically between the two experimental distributions of contact area (see Figure 4C)**.** Hence, we propose that the contact area between pairs of cells can influence the fate outcome of Notch-Delta signalling in the *Drosophila* midgut (Figure 4E), with small contact area clearly favouring symmetric self-renewal.

Discussion

We have considered a standard model of Delta/Notch-mediated lateral inhibition (Collier et al., 1996) and investigated the effect of the trans-activation of Notch by Delta and the inhibition threshold of Delta by Notch signalling (here considered phenomenologically as the thresholds a and b, respectively) on the dynamics of lateral inhibition for a system of two cells. We find that, provided there is a degree of variability in signalling thresholds between cell pairs, three different signalling states (and therefore fate combinations) can occur under the same conditions. This is a considerable

expansion of the model, whose use has so far been mostly centred on solutions that provide fine-grained (checkerboard) patterns. This population-level variability of signalling thresholds can be associated to diversity in the contact areas between pairs of cells. The model reproduces the signalling outcomes observed in the *Drosophila* intestine, which translate into differentiation vs. self-renewal fates. This in turn provides a mechanism whereby ISCs may undergo neutral competition, which is a widespread pattern of adult tissue maintenance in metazoans from *Drosophila* to humans. These results thus provide a potential biological justification for the neutral competition of *Drosophila* adult ISCs.

The seminal work by (Collier et al., 1996) established a minimal model which crystallised the biological intuition of lateral inhibition developed from the observation of neurogenesis and akin processes of precursor selection (Sprinzak et al., 2011; Formosa-Jordan et al., 2012; Petrovic et al., 2014): amplification of small differences in signal, leading to checkerboard patterns of stable, all-or-none signalling states. This formalisation, with their parameter choice for a, b, has justly become a reference in the field. In the last few years there have been expansions of this model to accommodate additional features, such as the specific activity of Jagged, another Notch ligand (Boareto et al., 2015), or departures from fine-grained patterns based on different ratios of positive and negative Notch cells (de Back et al., 2013). These models introduce additional genetic components or noise terms that allow the new phenomenology. By contrast, we have left intact the general dynamics of the minimal model of (Collier et al., 1996) and introduced only a degree of variability in the sensitivity of each cell pair to signal transduction.

Another important contribution of (Collier et al., 1996) et al. was to identify the mathematical condition for symmetry breaking. We explore this condition further and determine systematically the contribution of the signalling thresholds a and b to the condition of stability (Figure 2A). It would also be interesting to explore how variation in the cooperativity of the Notch trans-activation or Delta inhibition (parameters r, h) affect the capability of the system to arrive to symmetric or asymmetric steady states, as seen recently in Turing patterns (Diambra et al., 2015).

Our work considers the contact area between cells engaged in signalling as the source of variation in signalling threshold. Contact area can be an effective tuning parameter of a biological system (Khait et al., 2015), as it can integrate mechanical constraints into signalling, as it has been shown for cell density and proliferative control by the Hippo pathway (Schlegelmilch et al., 2011; Kim et al., 2011; Silvis et al., 2011) . In a system such as the posterior midgut, where some differentiated cells are much larger than their progenitors (see Figure 1A), differentiated and mature cell loss certainly would have a local impact in the packing geometry of cells interacting via Delta/Notch, and connect naturally with the fate outcome of stem cell divisions. This could be particularly useful in conditions of regeneration. Importantly, our theoretical framework could in principle accommodate any source of variation; for instance, variation arising from the unequal (either random or regulated) inheritance of signalling components could result in variation in the capability of signal transduction in the population. It is interesting to consider that while shortly after division the ISC daughter cells display similar levels of Notch and Delta proteins (Ohlstein and Spradling, 2006), endosomes bearing the signalling molecule Sara display an inhomogeneous inheritance pattern (Montagne and González-Gaitán, 2014).

Understanding how Notch/Delta signalling results in stochastic cell fate patterns is of particular relevance in adult homeostatic tissues, as Notch signalling controls fate in many types of tissue stem cells (Koch et al., 2013). Moreover, many adult stem cells balance their fate via neutral competition (Krieger and Simons, 2015). Our model proposes a mechanism whereby Notch/Delta signalling could result in neutral competition of stem cells by lateral inhibition between sibling cells. This provides an alternative explanation to the neutral competition of Drosophila adult ISCs, which has been proposed to arise from Notch/Delta-mediated lateral inhibition involving the offspring of non-related ISCs, coinciding in space (de Navascués et al., 2012) and resolving 20% of the time in symmetric fate. However, that proposal faces the difficulty that ISC/EB nests rarely contain more than two cells (de Navascués et al., 2012). Moreover, we and others have found isolated pairs of ISCs or EBs frequently in the tissue (de Navascués et al., 2012; Goulas et al., 2012). Our model provides a potential explanation of how the offspring of a single

ISC (pairs of Notch/Delta signalling cells) may reach a symmetric steady state, leading to symmetric self renewal o differentiation.

It would be interesting to see how our model (based on signalling threshold variability) translates to a larger group of interacting cells, in particular in light of recent findings in the esophageal epithelium. There, tissue is maintained by the neutral competition of basal progenitor cells (Doupé et al., 2012), and this competition is heavily influenced by Notch signalling, to the point that alterations in the pathway can lead to the fixation of mutant clones and poise the tissue for tumour initiation (Alcolea et al., 2014).

Acknowledgements

We wish to acknowledge support from CONICET to NG and from Cardiff University to JdN. JGO and RMC are supported by the Spanish Ministerio de Economía y Competitividad and FEDER, through project FIS2012-13360-C02-01, and the ICREA Academia Programme. RMC also acknowledges financial support from La Caixa Foundation. We would like to thank Alfonso Martínez Arias for his encouragement and support.

References

Alcolea, M. P., Greulich, P., Wabik, A., Frede, J., Simons, B. D. and Jones, P. H. (2014). Differentiation imbalance in single oesophageal progenitor cells causes clonal immortalization and field change. *Nature Cell Biology* **16**, 615–622.

Arias, A. M. and Stewart, A. (2002). *Molecular Principles of Animal Development*. Oxford University Press, USA.

Artavanis-Tsakonas, S., Rand, M. D. and Lake, R. J. (1999). Notch signaling: cell fate control and signal integration in development. *science (New York, NY)* **284**, 770–776.

Baker, A.-M., Cereser, B., Melton, S., Fletcher, A. G., Rodriguez-Justo, M., Tadrous, P. J., Humphries, A., Elia, G., McDonald, S. A. C., Wright, N. A., et al. (2014). Quantification of crypt and stem cell evolution in the normal and neoplastic human colon. *CellReports* **8**, 940–947.

Bardin, A. J., Perdigoto, C. N., Southall, T. D., Brand, A. H. and Schweisguth, F. (2010). Transcriptional control of stem cell maintenance in the Drosophila intestine. **137**, 705–714.

Biteau, B., Hochmuth, C. E. and Jasper, H. (2008). JNK activity in somatic stem cells causes loss of tissue homeostasis in the aging Drosophila gut. *Cell Stem Cell* **3**, 442–455.

Boareto, M., Jolly, M. K., Lu, M., Onuchic, J. N., Clementi, C. and Ben-Jacob, E. (2015). Jagged–Delta asymmetry in Notch signaling can give rise to a Sender/Receiver hybrid phenotype. *Proceedings of the National Academy of Sciences* **112**, E402–E409.

Bray, S. and Furriols, M. (2001). Notch pathway: making sense of suppressor of hairless. *Curr Biol* **11**, R217–21.

Collier, J. R., Monk, N. A., Maini, P. K. and Lewis, J. H. (1996). Pattern formation by lateral inhibition with feedback: a mathematical model of delta-notch intercellular signalling. *J Theor Biol* **183**, 429–446.

de Back, W., Zhou, J. X. and Brusch, L. (2013). On the role of lateral stabilization during early patterning in the pancreas. *Journal of The Royal Society Interface* **10**, 20120766.

de Navascués, J., Perdigoto, C. N., Bian, Y., Schneider, M. H., Bardin, A. J., Martinez-Arias, A. and Simons, B. D. (2012). Drosophila midgut homeostasis involves neutral competition between symmetrically dividing intestinal stem cells. *EMBO J* **31**, 2473–2485.

Diambra, L., Senthivel, V. R., Menendez, D. B. and Isalan, M. (2015). Cooperativity to increase Turing pattern space for synthetic biology. *ACS Synth Biol* **4**, 177–186.

Doupé, D. P., Alcolea, M. P., Roshan, A., Zhang, G., Klein, A. M., Simons, B. D. and Jones, P. H. (2012). A Single Progenitor Population Switches Behavior to Maintain and Repair Esophageal Epithelium. *science (New York, NY)* **337**, 1091–1093.

Ehebauer, M., Hayward, P. and Arias, A. M. (2006). Notch, a universal arbiter of cell fate decisions. *science (New York, NY)* **314**, 1414–1415.

Formosa-Jordan, P., Ibanes, M., Ares, S. and Frade, J. M. (2012). Regulation of neuronal differentiation at the neurogenic wavefront. *Development* **139**, 2321–2329.

Goulas, S., Conder, R. and Knoblich, J. A. (2012). The Par Complex and Integrins Direct Asymmetric Cell Division in Adult Intestinal Stem Cells. *Cell Stem Cell* **11**, 529–540.

Greenwald, I. (1998). LIN-12/Notch signaling: lessons from worms and flies. *Genes & Development* **12**, 1751–1762.

Khait, I., Orsher, Y., Golan, O., Binshtok, U., Gordon-Bar, N., Amir- Zilberstein, L. and Sprinzak, D. (2015). Quantitative analysis of Delta-like-1 membrane dynamics elucidates the role of contact geometry on Notch signaling. *cell reports* **In Press**, 1–27.

Kim, N.-G., Koh, E., Chen, X. and Gumbiner, B. M. (2011). E-cadherin mediates contact inhibition of proliferation through Hippo signaling-pathway components. *Proceedings of the National Academy of Sciences* **108**, 11930–11935.

Klein, A. M. and Simons, B. D. (2011). Universal patterns of stem cell fate in cycling

adult tissues. **138**, 3103–3111.

Koch, U., Lehal, R. and Radtke, F. (2013). Stem cells living with a Notch. **140**, 689–704.

Krieger, T. and Simons, B. D. (2015). Dynamic stem cell heterogeneity. **142**, 1396–1406.

Kullback, S. and Leibler, R. A. (1951). On Information and Sufficiency. *Ann. Math. Statist.* 79–86.

Maeda, K., Takemura, M., Umemori, M. and Adachi-Yamada, T. (2008). E-cadherin prolongs the moment for interaction between intestinal stem cell and its progenitor cell to ensure Notch signaling in adult Drosophila midgut. *Genes Cells* **13**, 1219–1227.

Micchelli, C. A. and Perrimon, N. (2006). Evidence that stem cells reside in the adult Drosophila midgut epithelium. *Nature* **439**, 475–479.

Miller, K. G., Field, C. M. and Alberts, B. M. (1989). Actin-binding proteins from Drosophila embryos: a complex network of interacting proteins detected by F-actin affinity chromatography. *The Journal of Cell Biology* **109**, 2963–2975.

Montagne, C. and González-Gaitán, M. (2014). Sara endosomes and the asymmetric division of intestinal stem cells. **141**, 2014–2023.

Muñoz-Descalzo, S., Tkocz, K., Balayo, T. and Arias, A. M. (2011). Modulation of the ligand-independent traffic of Notch by Axin and Apc contributes to the activation of Armadillo in Drosophila. *Development* **138**, 1501–1506.

LeVeque, R. J. (2007). Finite difference methods for ordinary and partial differential equations: steady-state and time-dependent problems (Vol. 98). *Siam*.

Ohlstein, B. and Spradling, A. (2006). The adult Drosophila posterior midgut is maintained by pluripotent stem cells. *Nature* **439**, 470–474.

Ohlstein, B. and Spradling, A. (2007). Multipotent Drosophila intestinal stem cells specify daughter cell fates by differential notch signaling. *science (New York, NY)* **315**, 988–992.

Othmer, H. G. and Scriven, L. E. (1971). Instability and dynamic pattern in cellular networks. *J Theor Biol* **32**, 507–537.

Petrovic, J., Formosa-Jordan, P., Luna-Escalante, J. C., Abello, G., Ibanes, M., Neves, J. and Giraldez, F. (2014). Ligand-dependent Notch signaling strength orchestrates lateral induction and lateral inhibition in the developing inner ear. *Development* **141**, 2313–2324.

Plahte, E. (2001). Pattern formation in discrete cell lattices. *J Math Biol* **43**, 411–445.

Quiñones-Coello, A. T., Petrella, L. N., Ayers, K., Melillo, A., Mazzalupo, S., Hudson, A. M., Wang, S., Castiblanco, C., Buszczak, M., Hoskins, R. A., et al. (2007). Exploring strategies for protein trapping in Drosophila. *Genetics* **175**, 1089–1104.

Rouault, H. and Hakim, V. (2012). Different Cell Fates from Cell-Cell Interactions: Core Architectures of Two-Cell Bistable Networks. *Biophysj* **102**, 417–426.

Sanders, P. G. T., Muñoz-Descalzo, S., Balayo, T., Wirtz-Peitz, F., Hayward, P. and Arias, A. M. (2009). Ligand-independent traffic of Notch buffers activated Armadillo in Drosophila. *PLoS Biol* **7**, e1000169.

Schlegelmilch, K., Mohseni, M., Kirak, O., Pruszak, J., Rodriguez, J. R., Zhou, D., Kreger, B. T., Vasioukhin, V., Avruch, J., Brummelkamp, T. R., et al. (2011). Yap1 acts downstream of α-catenin to control epidermal proliferation. *Cell* **144**, 782–795.

Shaya, O. and Sprinzak, D. (2011). From Notch signaling to fine-grained patterning: Modeling meets experiments. *Curr. Opin. Genet. Dev.* 1–8.

Silvis, M. R., Kreger, B. T., Lien, W.-H., Klezovitch, O., Rudakova, G. M., Camargo, F. D., Lantz, D. M., Seykora, J. T. and Vasioukhin, V. (2011). α-catenin is a tumor suppressor that controls cell accumulation by regulating the localization and activity of the transcriptional coactivator Yap1. *Science Signaling* **4**, ra33–ra33.

Simons, B. D. and Clevers, H. (2011). Strategies for homeostatic stem cell self-renewal in adult tissues. *Cell* **145**, 851–862.

Simpson, P. (2001). Notch signalling in development: on equivalence groups and asymmetric developmental potential. *Curr. Opin. Genet. Dev.* **7**, 537–542.

Sprinzak, D., Lakhanpal, A., LeBon, L., Garcia-Ojalvo, J. and Elowitz, M. B. (2011). Mutual Inactivation of Notch Receptors and Ligands Facilitates Developmental Patterning. *PLoS Comput Biol* **7**, e1002069.

Sprinzak, D., Lakhanpal, A., LeBon, L., Santat, L. A., Fontes, M. E., Anderson, G. A., Garcia-Ojalvo, J. and Elowitz, M. B. (2010). Cis-interactions between Notch and Delta generate mutually exclusive signalling states. *Nature* **465**, 86–90.

Tepass, U., Tanentzapf, G., Ward, R. and Fehon, R. (2001). Epithelial cell polarity and cell junctions in Drosophila. *Annu Rev Genet* **35**, 747–784.

Vermeulen, L. and Snippert, H. J. (2014). Stem cell dynamics in homeostasis and cancer of the intestine. *Nat Rev Cancer* 1–13.

Vermeulen, L., Morrissey, E., van der Heijden, M., Nicholson, A. M., Sottoriva, A., Buczacki, S., Kemp, R., Tavaré, S. and Winton, D. J. (2013). Defining stem cell dynamics in models of intestinal tumor initiation. *science (New York, NY)* **342**, 995–998.

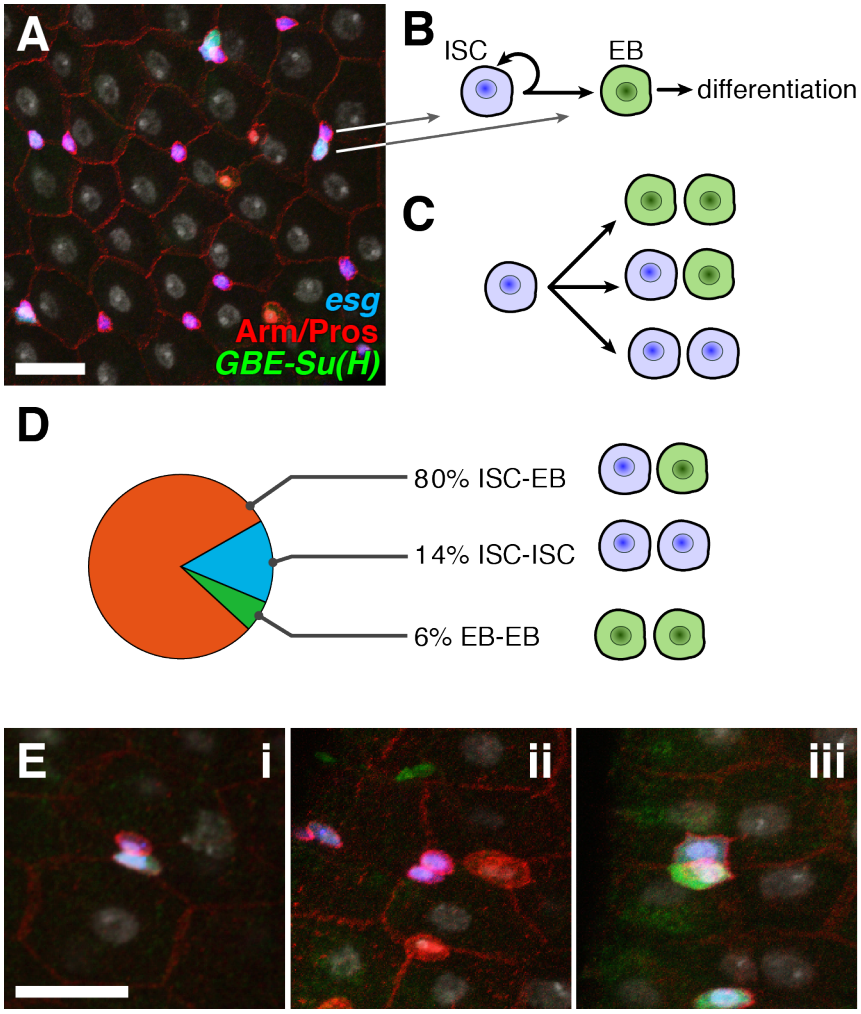

Figure 1. Tissue maintenance in the *Drosophila* adult midgut. Scale bars: 20μm. **A.** Confocal micrograph showing the cell types present in the midgut epithelium. ISCs are esg-GFP$^+$ (blue) and EBs are esg-GFP$^+$ and GBE-Su(H)-lacZ$^+$ (green). The two differentiated cells, enteroendocrine cells and enterocytes, are recognisable by Prospero (pros) expression and having large, polyploid nuclei (Hoechst, grey), respectively. **B-C.** ISCs self renew and produce EBs (which will terminally differentiate without further division) (B), by dividing either asymmetrically (one ISC and an EB), or symmetrically into two ISCs or two EBs (C). **D.** Distribution of cell fates for nests containing two undifferentiated cells (N=508). ISC-ISC pairs (blue, N=74), EB-EB pairs (green, N=28) and ISC-EB pairs (orange, N=406). **E.** Confocal micrographs showing examples of cell pair fate profiles: asymmetric (i), symmetric Notch negative (two ISCs, ii) and symmetric Notch positive (two EBs, iii).

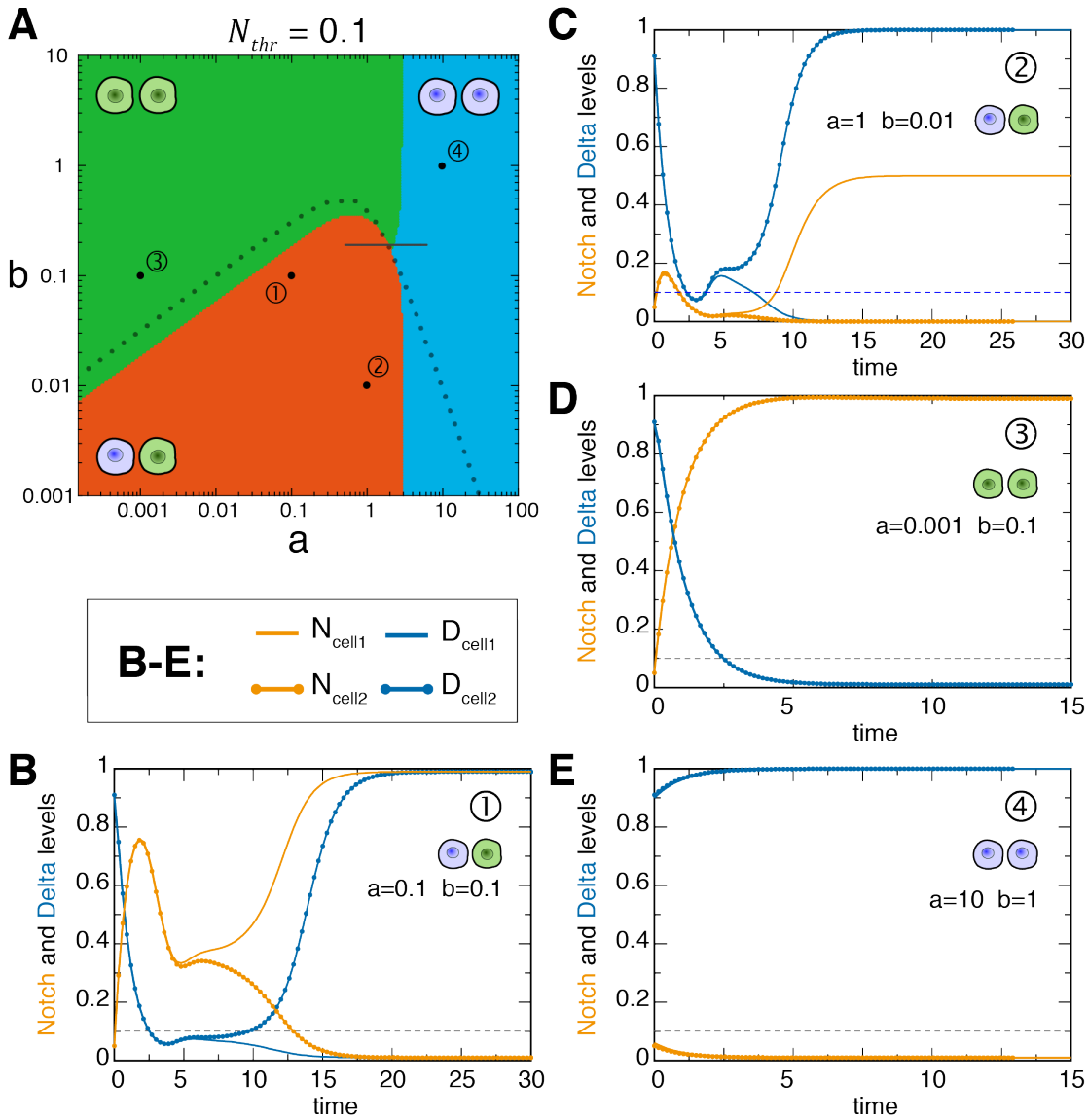

Figure 2. Parameter space and dynamic behaviour of the model. **A.** Stable solutions of the system classified according to their resulting signalling state. Green stands for symmetric positive fates (EB-EB pairs), blue represents symmetric negative fates (ISC-ISC pairs), and orange denotes asymmetric fates (ISC-EB pairs). The threshold in Notch level for EB identification is taken to be equal to 0.1 (see the text for more details). The short, horizontal line indicates 95% of "a" values used to generate a theoretical distribution of cell fates for b=0.19 (see main text). Dotted line, boundary of stability for steady states with identical cells; these 'homogeneous' solutions are stable above the line. **B-E.** Time evolution (in arbitrary units) of Notch and Delta activity in pairs of cells interacting with parameters from the points indicated as 1 to 4 in (A). For the calculations, we are considering $r = h = 2$ and $\delta_N = \delta_D$, as in previous works (Collier et al., 1996; Sprinzak et al., 2010). Parameter values in point 1 correspond to those used in Collier et al. (1996) (B), while parameter values in points 2-4 (C-E) correspond to examples of other asymmetric pairs, and symmetric positive and symmetric negative pairs.

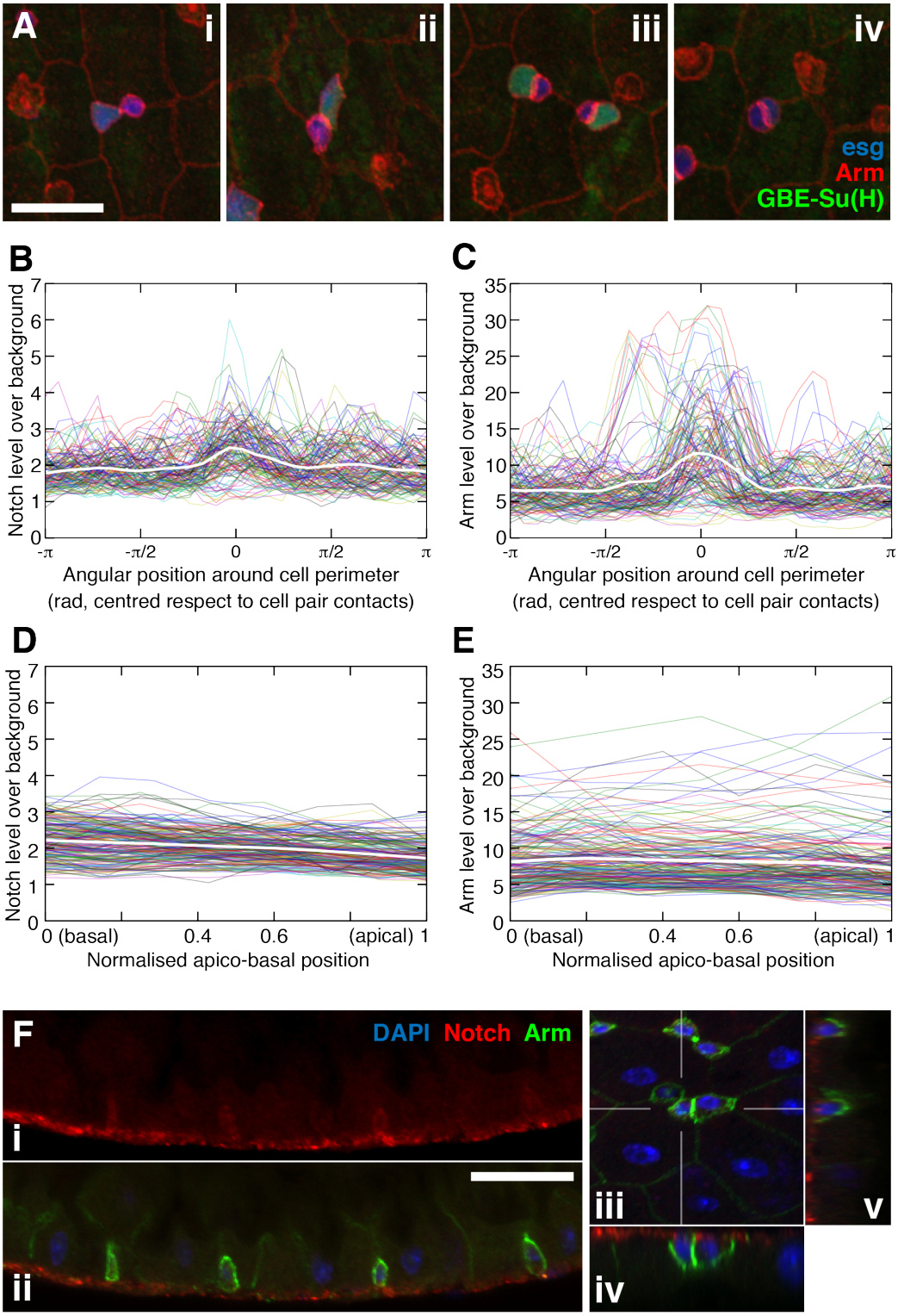

Figure 3. Variability in contact area and distribution of Notch at the membrane. **A.** Confocal stacks projected in Z, showing variability in contact length (as proxy for area). Scale bar: 20μm. **B-C.** Notch (B) and Arm (C) levels along the perimeter of the cell planes (colour lines) and mean (white). For each cell plane, position 0 corresponds to the centre of the contacting membranes (defined as the position that intersects the line connecting the cell centroids in that plane). **D-E.** Notch (D) and Arm (E) levels along the apical-basal cell axis (with height of the cell normalised to 1). Each cell contributes ten lines to the plot, corresponding to the intensity values along the vertical axis of non-overlapping, angular windows of 2π/10. Data displayed in B-E are from 20 paired esg$^+$ cells. Data in B-E are from 20 paired cells. **F.** Side views of the intestinal epithelium, showing apical-basal distribution of Notch and Arm. Lumen is at the top and basal at the bottom. Scale bar: 10μm.

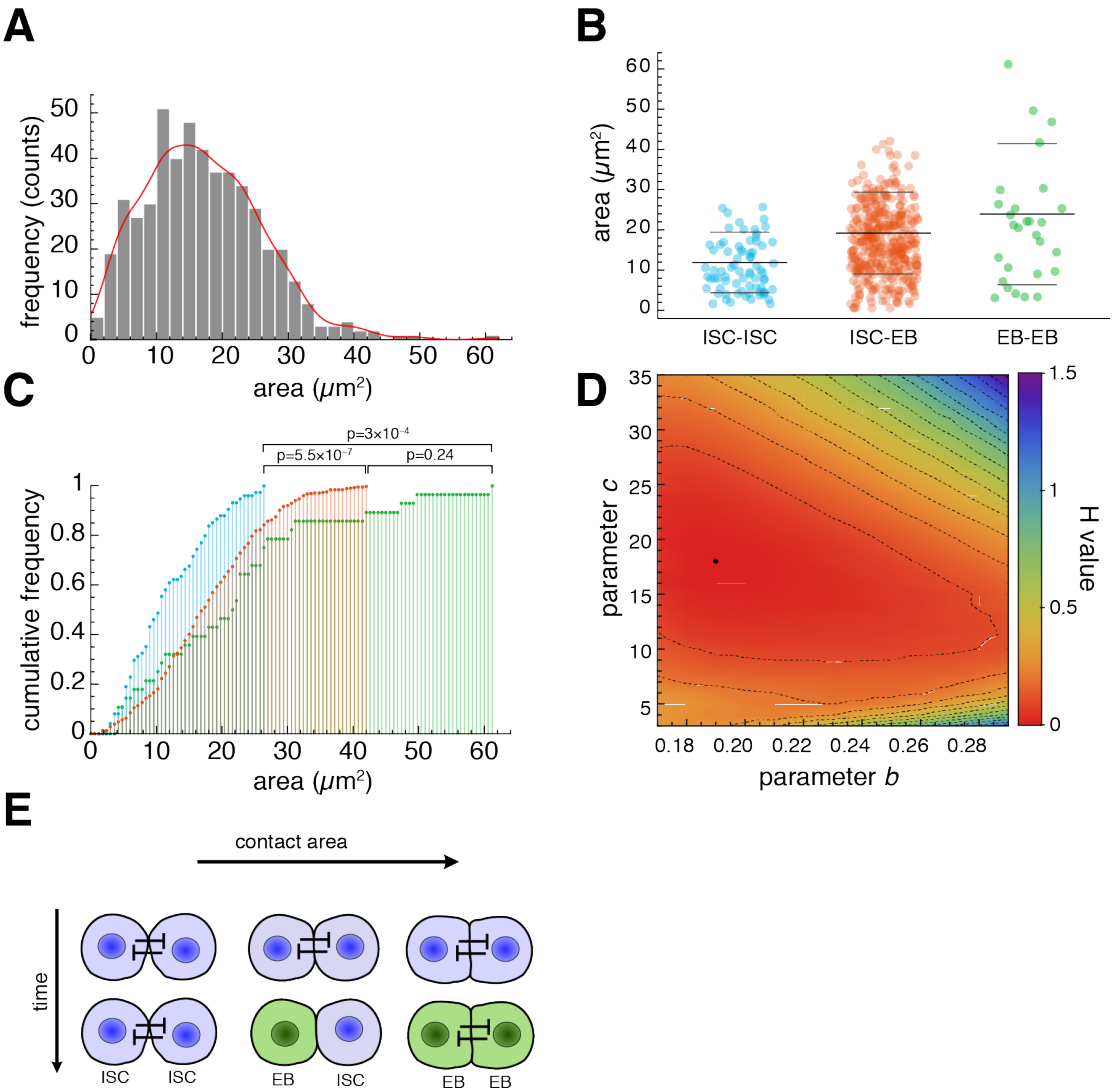

Figure 4. The model can reproduce the observed cell fate profiles. Data set from N=508 nests (Figure 1D). **A.** Frequency of contact area values for nests of two undifferentiated cells. Line marks the Smooth Kernel Distribution (SKD) used to generate areas for the simulation. **B.** Contact area values segregated by fate profiles. Lines indicate mean values. **C.** Cumulative frequency of the contact area data displayed in (B). Note ISC-EB and EB-EB distributions cannot be distinguished statistically. **D.** Kullback-Leibler relative entropy (*H*) between experimental and model distributions as a function of *b* and *c*. Values of area in the model are generated by the SKD depicted in (A). Best value corresponds to *b*=0.19 and *c*=18 (black dot) and leads to fate profile proportions as in Table 1. **E.** Fate outputs for the lateral inhibition model for three different values of the contact area.

Table 1. Cell-fate profiles as obtained experimentally and theoretically. The value of Kullback-Leibler relative entropy between the two distributions is 0.3×10^{-3}. Model parameters: b=0.19 and c=18.

pair fate	experimental	model
ISC-ISC	14.6 %	15.1%
EB-EB	5.5 %	5.0 %
ISC-EB	79.9 %	79.9%

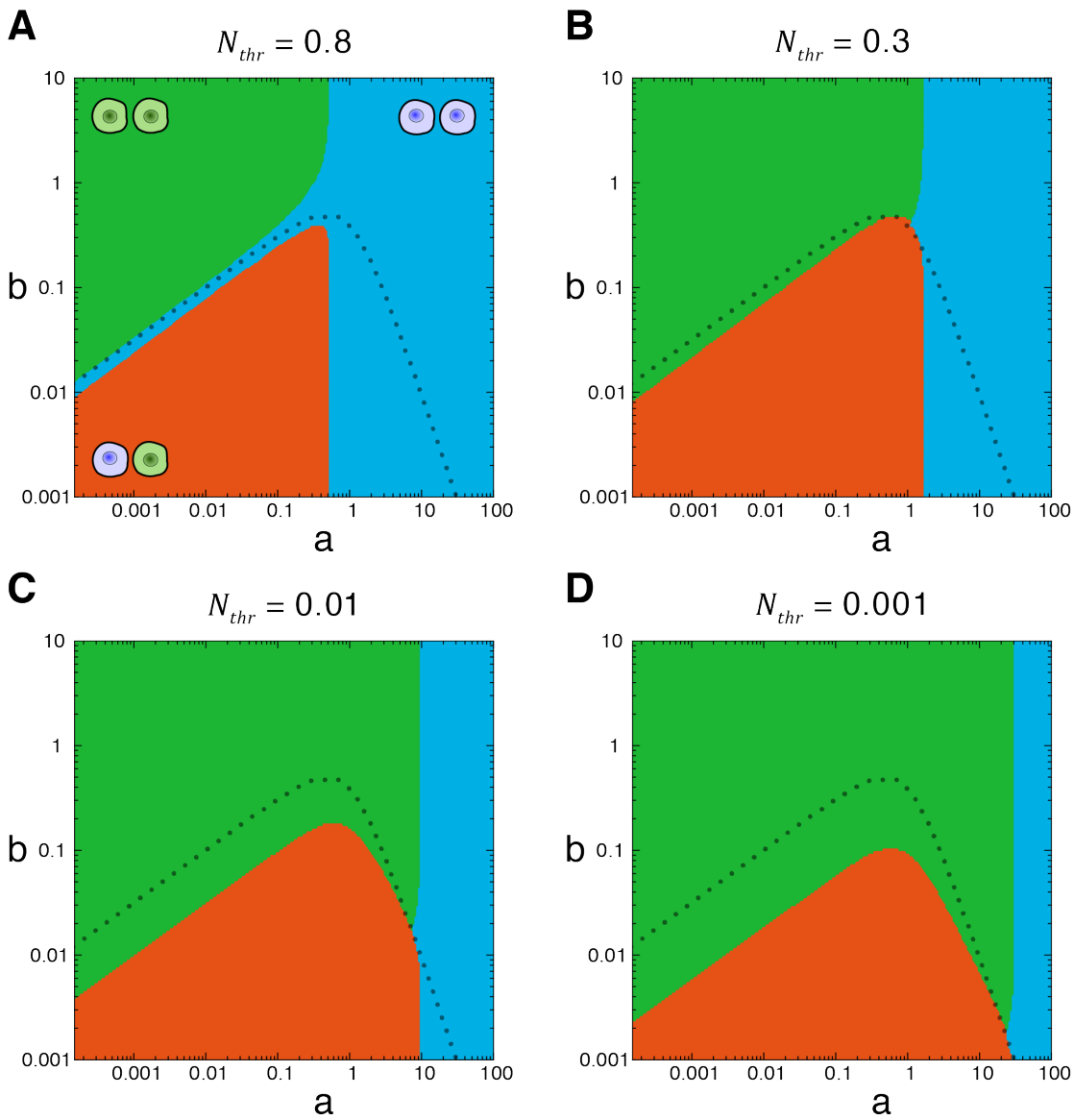

Supplementary Figure 1. Fate profiles in parameter space over a broad range of threshold N_{thr} values. **A-D.** Phase space for N_{thr} equal to 0.8 (A), 0.3 (B), 0.01 (C), and 0.001 (D), respectively. The dotted line marks the stability boundary for the 'homogeneous' solutions (pairs of identical cells), and serves as reference for comparison with Figure 2A. While in A (where $N_{thr} > 0.7$), the area of asymmetric fate is surrounded by symmetric negative resolution, in B-D the organisation of the phase space is very similar, with the transitions shifting along the stability boundary.

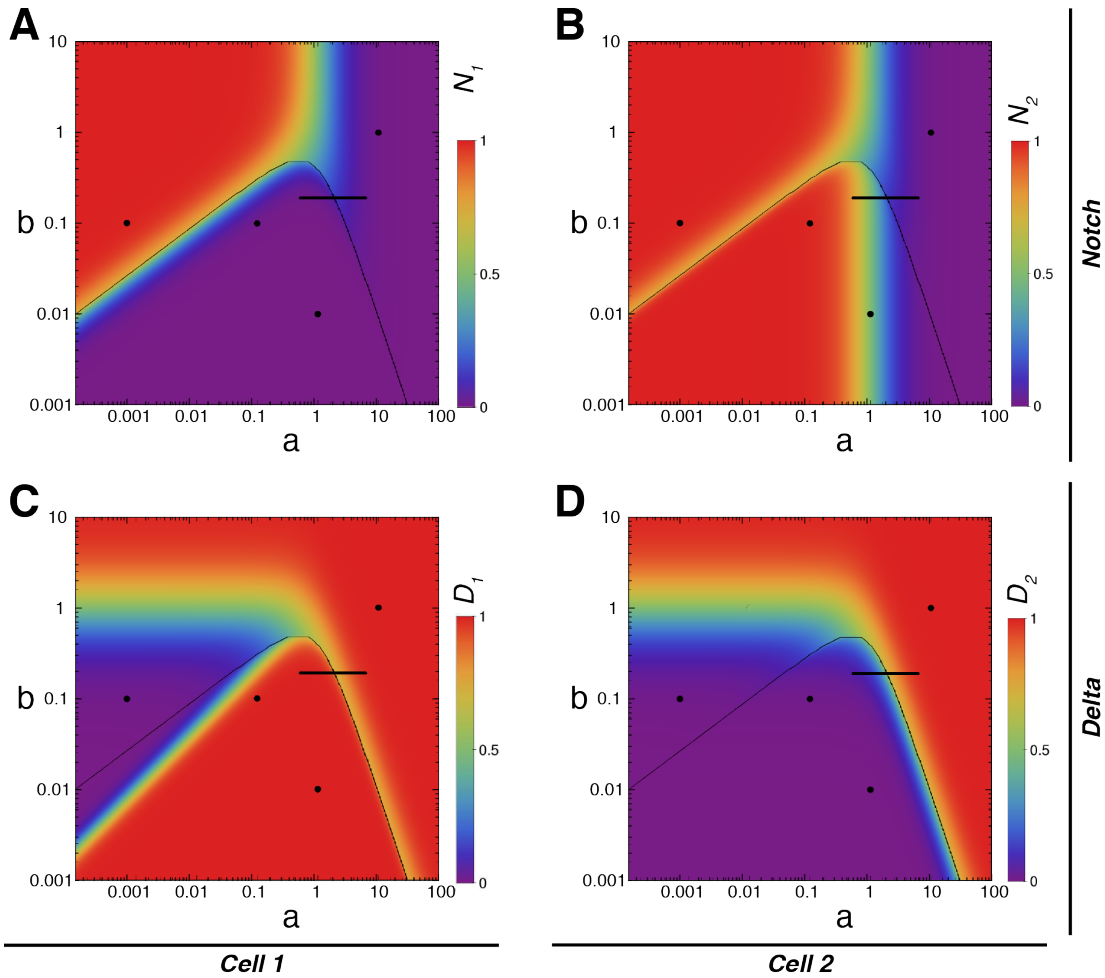

Supplementary Figure 2. Values of Notch and Delta at steady state across parameter space. The short, horizontal line indicates 95% of "a" values used to generate a theoretical distribution of cell fates for b=0.19 (see main text). Dotted line, boundary of stability for steady states with identical cells. The black dots mark the parameter values used in (Collier et al., 1996) (Figure 2B) and the asymmetric, symmetric positive and symmetric negative pairs from Figure 2C-E. **A, B.** Steady-state values of activated Notch the two cells of a pair (one in each panel) respect to a, b. **C-D.** Steady-state values of Delta in the two cells of a pair (one in each panel) respect to a, b. Note that depending on the value of activated Notch, one can find symmetric negative or symmetric positive fate profiles below the boundary (region of heterogeneous solution), showing that the model allows for symmetric steady states where cells in a pair do not have identical amounts of N or Dl.

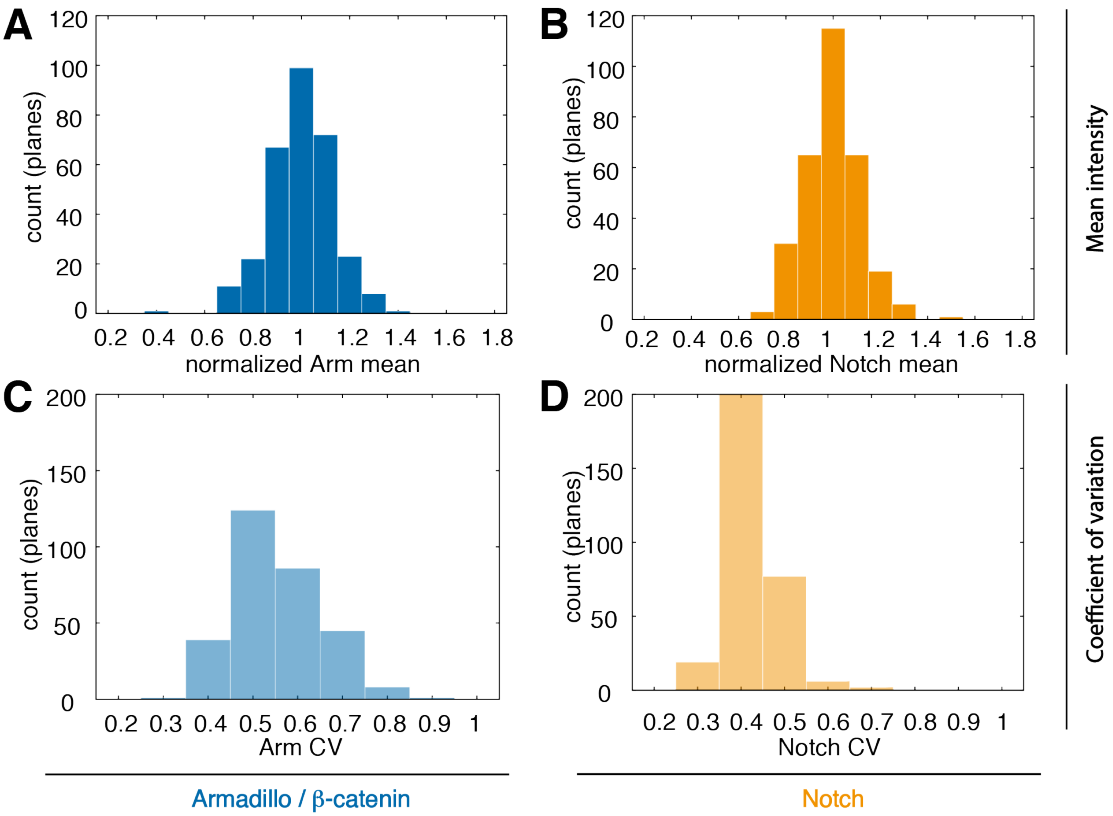

Supplementary Figure 3. Distribution of Notch and Armadillo at the membrane. Data correspond to all 51 analysed cells (single and paired). **A-D.** Histograms of the normalised mean intensity per plane (A, B) and the coefficient of variation (CV) per plane (C, D) for Notch (A, C) and Armadillo (B, D) markers. The normalised mean intensity in plane *i* is defined as the ratio of the average of the plane and the average for the cell: $<Inty_{plane}>/<Inty_{i\text{-}th\ cell}>$.